ELSEVIER

Journal of Alloys and Compounds 224 (1995) 101–107

Journal of ALLOYS AND COMPOUNDS

Magnetic properties of several Ce_2T_2M phases with T = Ni, Pd and M = In, Sn, Pb

R.A. Gordon, Y. Ijiri, C.M. Spencer, F.J. DiSalvo *

Department of Chemistry, Cornell University, Ithaca, NY, 14853-1301, USA

Received 28 November 1994

Abstract

Four new ternary intermetallic compounds were prepared: Ce_2Pd_2In, Ce_2Pd_2Sn, Ce_2Pd_2Pb and Ce_2Ni_2Sn. The first three are isotypic, adopting the tetragonal U_3Si_2 structure. The structure of Ce_2Ni_2Sn is of the orthorhombic Mo_2CoB_2 type, but extensive solid solutions occur between it and Ce_2Pd_2Sn. Magnetic susceptibility measurements were performed on each ternary and the known Ce_2Ni_2In phase. Cerium is tetravalent in Ce_2Ni_2In and trivalent in the remaining phases at room temperature. Kondo behaviour is present in Ce_2Ni_2Sn with T_K near 9 K. Ferromagnetic behaviour with T_c near 4.2 K is seen in both Ce_2Pd_2In and Ce_2Pd_2Sn. Anti-ferromagnetic ordering is observed in Ce_2Pd_2Pb with a Néel temperature of 6.2 K. An apparently second-order transition involving a reduction in the effective cerium moment also occurs in Ce_2Pd_2Pb at 120 K.

Keywords: Cerium intermetallics; Magnetic susceptibility

1. Introduction

The presence of the 4f level near the Fermi level in cerium intermetallics can give rise to some unusual electronic effects. Intermediate valent, heavy fermion, Kondo lattice or Kondo insulator behaviour has been observed in the Ce–Ni–Sn(In) and Ce–Pd–Sn(In) ternary systems [1–5]. While searching the Ce–Pd–Sn system for new materials exhibiting these types of behaviour [6], we found the ternary Ce_2Pd_2Sn. Since complete solid solutions are obtained when Pd is replaced by Ni in both CePdSn and CePd [1,7], we attempted substitution of Ni for Pd and In or Pb for Sn. Ferromagnetic CePd becomes mixed-valent CeNi on substitution [7]. Anti-ferromagnetism and heavy fermion behaviour are observed in CePdSn but, on Ni substitution, a Kondo insulator is obtained [1]. Similar changes in the interaction between the Ce 4f level and conduction states were anticipated here.

2. Experimental procedure

Samples were prepared by arc melting of the elements in the desired ratio under flowing argon, gettered in a titanium purifier (Centorr Furnaces, Model 2B-20) on a tantalum-coated, water-cooled, copper hearth. Elements used were at least of 99.9% purity. The cerium was first melted under vacuum and allowed to drip into a water-cooled copper cup. This was done for ease of cutting with heavy-wire cutters and helped to reduce ferromagnetic impurities that are often present after sawing Ce into pieces. Mass losses after arc melting were less than 0.5% for all but the Pb sample. Owing to the high vapour pressure of Pb, a small excess (ca. 1%) was added. The final masses of Pb-containing samples were within 0.5% of what would be the stoichiometric values. Annealing was accomplished by placing the samples in sections of tantalum tubing, then sealing in quartz under vacuum. Samples were annealed for either 3 weeks at 750 °C or 4 weeks at 700 °C. All were brittle, with Ce_2Pd_2In, Ce_2Pd_2Sn and Ce_2Ni_2Sn showing a tendency to crack macroscopically on cooling to room temperature in the arc furnace.

Powder diffraction data on annealed and unannealed material were obtained using a Scintag XDS 2000 diffractometer and analyzed using the programs TREOR [8] and LATCON-Z, a least-squares lattice parameter refinement program. Magnetic measurements were performed by the Faraday technique on coarsely ground, loose powder. Platinum was used as a calibration standard. Field dependence of the susceptibility of all samples was examined from 2.1 to 14.6 kG at room temperature to check for ferromagnetic impurities. Vari-

* Corresponding author.

SSDI 0925-8388(94)01510-4

ations of 2% or less in susceptibility were observed in all cases. Data were collected, typically, using a field of 10 kG. Resistance measurements, where reported, were performed using standard four-probe techniques.

3. Results and discussion

The X-ray powder patterns for Ce_2Ni_2In [9], Ce_2Pd_2In, Ce_2Pd_2Sn and Ce_2Pd_2Pb can be indexed to a tetragonal cell with similar lattice parameters (Table 1). Calculated intensities based on the atomic positions of U_2Rh_2Sn (U_3Si_2 structure type, space group *P4/mbm*) [10] using LAZY-PULVERIX [11] were compared with the experimental patterns and showed satisfactory agreement (Table 2). No particular attempt was made to prepare powdered X-ray samples with particle sizes under 10 μm, so some deviation of the observed intensities from the calculated is expected [12]. The pattern for Ce_2Ni_2Sn indexed to an orthorhombic cell with lattice parameters similar to those for Ce_2Ni_2Ga and Y_2Ni_2Ga (Mo_2CoB_2 structure, space group *Immm*) [13]. Again, a comparison between experimental and calculated intensities, based on the positions for Y_2Ni_2Ga, shows a reasonable agreement. X-ray patterns of unannealed samples, although not as sharp as those for annealed material, strongly resemble them, suggesting that these ternaries may be congruently melting or nearly so.

Table 1
Lattice parameters for Ce_2T_2M phases with T = Ni, Pd and M = In, Sn, Pb, with literature values for Ce_2Ni_2In from Ref. [9]

Phase	*a*/Å	*b*/Å	*c*/Å	Volume/Å^3
Ce_2Ni_2Sn	5.735(2)	8.591(3)	4.391(1)	216.3
Ce_2Ni_2In [9]	7.499(2)		3.751(2)	210.9
Ce_2Ni_2In	7.526(1)		3.722(1)	210.8
Ce_2Pd_2In	7.805(1)		3.913(1)	238.3
Ce_2Pd_2Sn	7.774(1)		3.926(1)	237.3
Ce_2Pd_2Pb	7.915(1)		3.872(2)	242.6

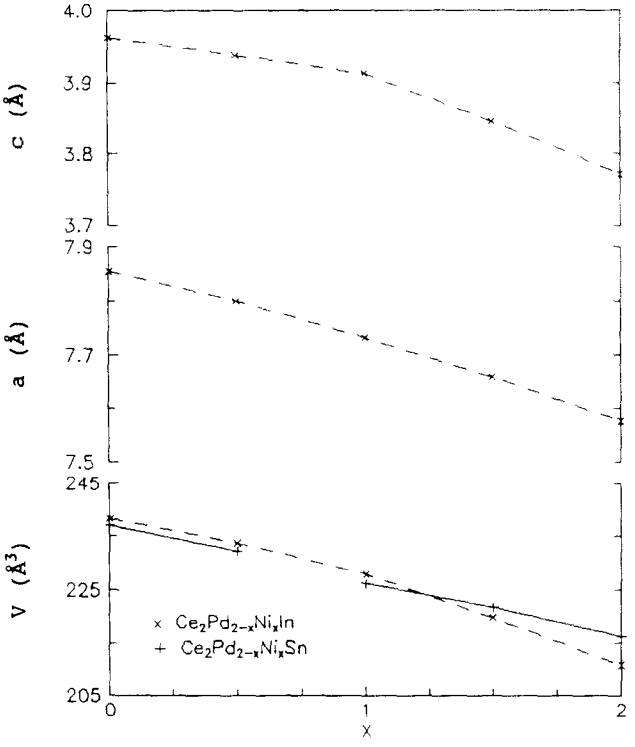

Fig. 1. Cell volume as a function of nickel content in $Ce_2Ni_xPd_{2-x}M$ with M = In, Sn, and lattice constants for M = In.

Both the Pd–In and Pd–Sn phases possess an extensive homogeneity range of the form $Ce_2Pd_{2+x}Sn_{1-y}$, for example, which will be discussed elsewhere [6]. On substitution of Ni for Pd in the Sn-containing compounds, there is a change in structure that occurs between 25% and 50% Ni. The dependence of cell volume on Ni concentration is shown in Fig. 1 for both the Sn and In materials. The variation in lattice constants is also shown for substitution between the isotypic In-containing ternaries.

Fig. 2 shows the magnetic susceptibility for each of the Ce_2T_2M phases being discussed as a function of temperature (heating) between 4.2 and 300 K. Also displayed are the inverse susceptibilities, when appropriate, for cooling and heating over the same temperature range. The results for fitting the heating data to the Curie–Weiss law:

$$\chi = \chi_0 + \frac{C}{T-\theta} \tag{1}$$

are given in Table 3 and will be discussed below. Fitting was achieved by selecting a temperature range of the fit, fixing θ, then determining C and χ_0 using standard data reduction techniques [14]. A range of θ values was used, and for each a fractional variance,

$$\sigma = \sqrt{\frac{1}{N}\sum_{1}^{N}\left(\frac{\chi_i - \chi_0 - \dfrac{C}{T_i-\theta}}{\chi_i}\right)^2} \tag{2}$$

was calculated. The best-fit parameters are those which minimized the fractional variance over the largest temperature range.

For Ce_2Pd_2In, Ce_2Pd_2Sn, Ce_2Ni_2Sn and, albeit less often, Ce_2Pd_2Pb, the susceptibilities on cooling exhibited discontinuities involving an increase in χ, resulting in some hysteretic-like behaviour. These jumps are most easily seen in χ^{-1}. Examples from Ce_2Pd_2In and Ce_2Pd_2Sn are shown in Fig. 2(e) and 2(g), respectively. We believe the discontinuities result from re-orientation of the loose powder samples in the magnetic field. Crystal field effects and spin–orbit coupling can produce anisotropy of the moment in non-cubic materials. Sechovský et al. [15] have expressed the possibility of this occurring in the related U_2T_2M materials. Anisotropy has been observed in $CeCoGe_3$ by the Faraday technique

Table 2
Comparison of calculated and observed peak intensities from X-ray powder diffraction patterns for $Ce_2(Ni,Pd)_2(In,Sn,Pb)$ phases

hkl [a]	Ce_2Pd_2In		Ce_2Pd_2Sn		Ce_2Pd_2Pb		*hkl* [a]	Ce_2Ni_2Sn	
	I_{calc}	I_{expt}	I_{calc}	I_{expt}	I_{calc}	I_{expt}		I_{calc}	I_{expt}
001	2	–	2	2	6	5	011	8	8
111	4	3	4	2	15	10	101	13	14
201 }	28	27	28	38	47	69	200	18	20
220 }	10		10		18	28	121	100	100
211	100	100	100	100	100	100	130	34	25
310	44	27	44	31	66	73	031	12	9
221	0.4	–	0.4	–	3	3	220	12	11
320	6	6	5	8	6	9	211	48	41
311	5	6	5	6	15	19	002	27	13
002	15	10	16	8	19	9	040	10	8
321 }	3		3		3	7	310	1	4
410 }	5	10	5	8	6	10	301	4	–
330	6	7	6	3	3	4	202	9	8
420	4	5	5	3	9	8	240	1	–
411	14	16	14	14	14	11	132	19	8
331	6	9	6	5	11	14	150	2	3
222	4	4	4	–	7	4	321	14	8
312	20	16	20	10	30	12	222	7	–
322	3	4	3	3	3	4	051	7	6
511	9	14	9	9	16	14	330	12	6
440	4	5	4	–	6	4	042	7	5
521	13	17	13	6	13	9	400 }	6	3
530	2	5	2	1	4	–	060 }	3	
422	3	–	4	–	7	5	251	25	9
441	4	–	4	–	6	12	123	12	5
600	4	13	5	4	7	5	213 }	7	
531	2	4	2	2	0.4	–	332 }	12	6
213	10	7	10	3	9	4	402	7	–

[a] A brace indicates two peaks which were not adequately resolved.

Table 3
Summary of magnetic data for Ce_2T_2M ternaries

Phase	μ_{eff}/μ_B	θ/K	T_c, T_N/K	σ (10^{-3})	Fit range/K
Ce_2Ni_2In	–	–	–	–	–
Ce_2Ni_2Sn	2.46(3)	10(2)	–	3.0	90–300
Ce_2Pd_2In	2.48(3)	18(2)	~4.2	2.3	80–320
Ce_2Pd_2Sn	2.62(2)	18(1)	~4.2	3.0	75–300
Ce_2Pd_2Pb	2.70(2)	−30(2)		1.7	140–300
Ce_2Pd_2Pb	2.37(3)	−1(1)	6.2	2.4	20–110

[16] using powder oriented in epoxy. If the anisotropy is sufficiently large, then small crystalline particles will experience a torque, forcing them to re-orient in the magnetic field if they are free to move. As the temperature is lowered, the torque increases, since the effective moments also increase, in general. Since the samples measured are polycrystalline, possibly with some preferred orientation due to directional solidification in the arc furnace, complete orientation of all single-crystal grains by the magnetic field is not assured. The data obtained on heating, however, do not exhibit discontinuous jumps, indicating that the orientation of the individual particles remained fixed on heating. Since we extract moments from these data, they are not average moments expected from a randomly oriented powder that we obtain, but rather ones closer to the maximum oriented moments. We also note that, when the temperature is of the order of the crystal field splitting, the moment becomes temperature dependent. When $T \gtrsim \Delta/k_B$, where Δ is the crystal field splitting and k_B is Boltzmann's constant, the susceptibility for a single ion can be fit reasonably well by a Curie–Weiss curve where θ is proportional to Δ [17]. Consequently, the high-temperature Weiss constant in rare earth (RE) compounds with close RE–RE distances may have contributions both from exchange and crystal field effects (i.e. $\theta \approx \theta_{exchange} + \theta_{crystal\ field}$).

3.1. Ce_2Ni_2In

The susceptibility curve for Ce_2Ni_2In (Fig. 2(a)) does not possess Curie behaviour below room temperature. A small amount of residual oxygen gas freezing in the Faraday system produced the anomaly at 50 K, and the small rise below 50 K is presumably due to a paramagnetic impurity in the sample. In this material,

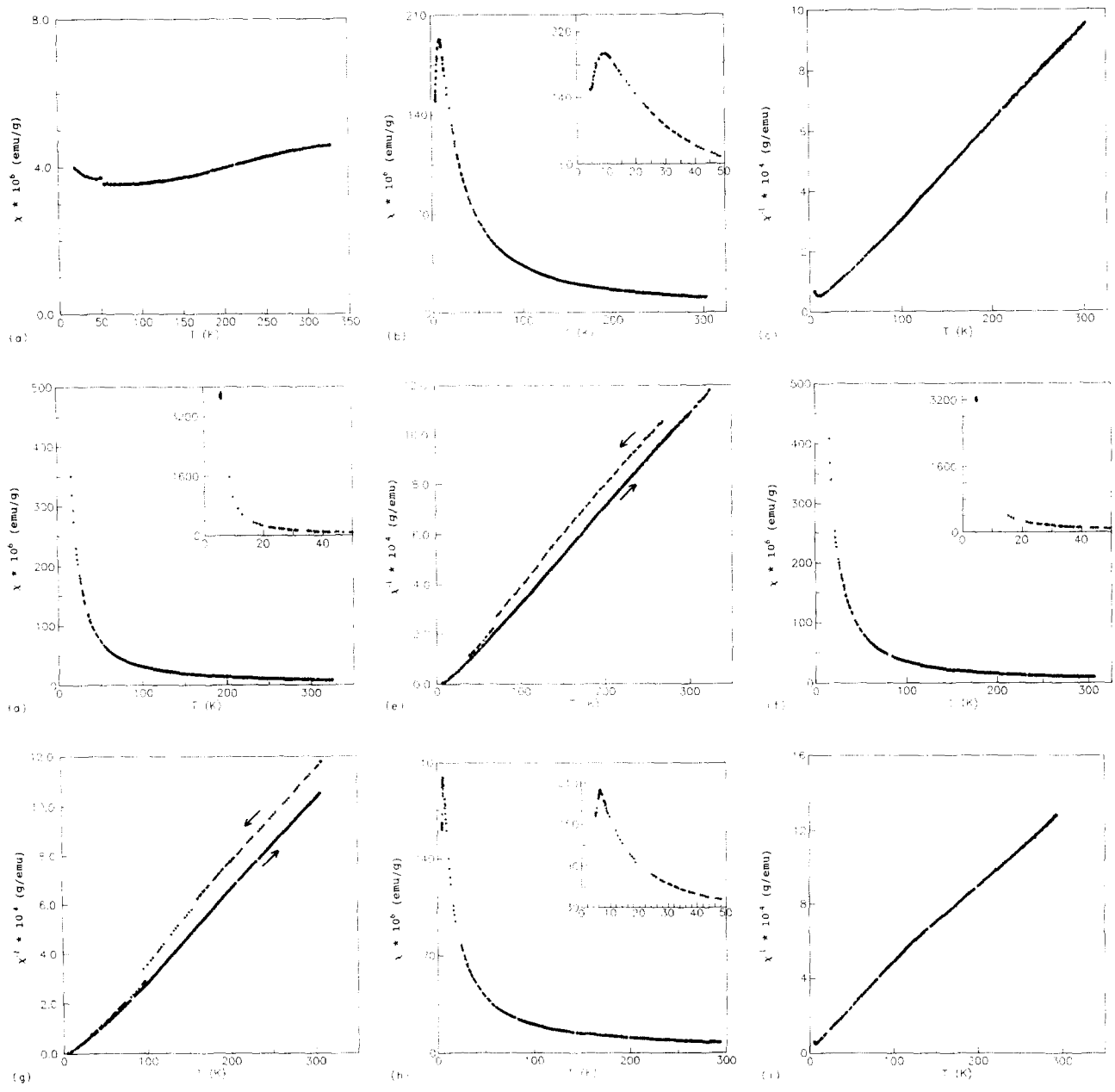

Fig. 2. Magnetic susceptibilities and inverse susceptibilities for (a) Ce_2Ni_2In, (b) and (c) Ce_2Ni_2Sn, (d) and (e) Ce_2Pd_2In, (f) and (g) Ce_2Pd_2Sn and (h) and (i) Ce_2Pd_2Pb.

the cerium valence is 4+ (or, equivalently, the temperature range for a Kondo interaction, T_K, is greater than 300 K).

From Fig. 1, the volume change on Ni substitution in Ce_2Pd_2In is greater than that for the Pd–Sn compound. The dependence of cell volume on the amount of Ni included deviates from linearity near 50% Ni. Extrapolating the two most Pd-rich points yields a hypothetical volume of 219.7 Å^3 for $Ce^{(3+)}{}_2Ni_2In$, versus the observed 210.8 Å^3. This additional decrease in volume is largely due to the change in the *c*-axis length. In the uranium compounds of composition U_2T_2M [18], it was observed that the *a* lattice spacing correlates with the size of the transition element. The almost linear dependence of *a* on the amount of Ni supports that observation. The *c* parameter was suggested to be affected by changes in the electronic structure. That, and the lack of an observable moment below 300 K, suggest that the Fermi level has dropped below the $4f^1$ energy level, resulting in the loss of a local Ce moment and a reduction in the effective size of the Ce atoms. Given that both CeNi and CeNiIn are mixed valent materials, one would expect the $4f^0$ level in Ce_2Ni_2In to lie just above ϵ_F. This could explain the unusual decrease in its susceptibility with decreasing temperature.

If one interprets the susceptibility to be due to Pauli paramagnetism, then, per mole of $CeNiIn_{0.5}$, one obtains a value of approximately 1×10^{-3} emu mol^{-1}. Owing

to a high density of states near ϵ_F, palladium metal has a large molar Pauli susceptibility of about 0.5×10^{-3} emu mol^{-1} at 300 K, and reaches a maximum of ca. 0.8×10^{-3} emu mol^{-1} at a lower temperature [19]. This suggests that a very high density of states exists in Ce_2Ni_2In, possibly due to mixing of the 4f orbitals with conduction states, or to a large Van Vleck susceptibility due to the presence of the $4f^0$ level near but above the Fermi level or, finally, to a strong Stoner enhancement of the Pauli susceptibility due to e^-–e^- interactions [20,21].

3.2. Ce_2Ni_2Sn

For Ce_2Ni_2Sn, Curie–Weiss behaviour is observed (Fig. 2(b) and (c)) from room temperature down to approximately 90 K with a slightly reduced moment of 2.46 μ_B when compared with the theoretical Ce^{3+} value of 2.54 μ_B. Attempts to broaden the range of fit to include data from lower temperatures resulted in an increased fractional variance, indicating behaviour more complex than a simple Curie–Weiss model describes (e.g. due to crystal field splitting of the $^2F_{5/2}$ free ion state). Weak ferromagnetic exchange ($\theta=10$ K) is suggested by fitting the susceptibility between 90 and 300 K. In this case, the broad peak at 9 K is unlikely to be due to anti-ferromagnetic ordering. A visual comparison of the peak shapes shown in the insets to Fig. 2(b) and (h), which shows anti-ferromagnetic ordering in Ce_2Pd_2Pb, supports this conclusion.

Further examination of this feature by resistance measurements was attempted. By repeated thermal cycling of a roughly 10 mm×2 mm×2 mm bar, reproducible resistance data were obtained. Cracks present in the arc-cast samples apparently continue to grow on cooling below room temperature but, on thermal cycling, most stress in the sample was relieved and consistent heating and cooling data could be obtained. Fig. 3 shows the last two cycles, which overlap, plotted on a logarithmic temperature scale up to 50 K. Since the sample contains cracks, an absolute resistivity cannot be calculated. A maximum is observed at approximately the same temperature as the peak in the susceptibility. At temperatures just above this peak, the resistance shows some linear dependence on log T, consistent with a Kondo interaction. Both the peak in the susceptibility and that in the resistance may be due to the Kondo effect. This would suggest Ce_2Ni_2Sn is a dense Kondo system.

3.3. Ce_2Pd_2In

This material shows (Fig. 2(d) and (e)) simple Curie-Weiss behaviour down to 80 K with a moment of 2.48 μ_B and Weiss constant of 18 K. A very small deviation from the Curie–Weiss law (apparent by sighting along the χ^{-1} vs. T curve in Fig. 2(e)) below 80 K is, again, presumably due to interactions not described by a simple Curie–Weiss model, and is probably due to crystal field effects. A measurement of field dependence at 4.2 K is shown in Fig. 4. Linear dependence on the inverse of the applied field is evident at higher fields, indicating ferromagnetism. From χ^{-1}, we can only estimate a T_c near 4.2 K. Although the high-temperature moment appears slightly reduced in Ce_2Pd_2In, χ exhibits no unusual behaviour, apart from the ferromagnetism. The Ce atoms are essentially in a trivalent state.

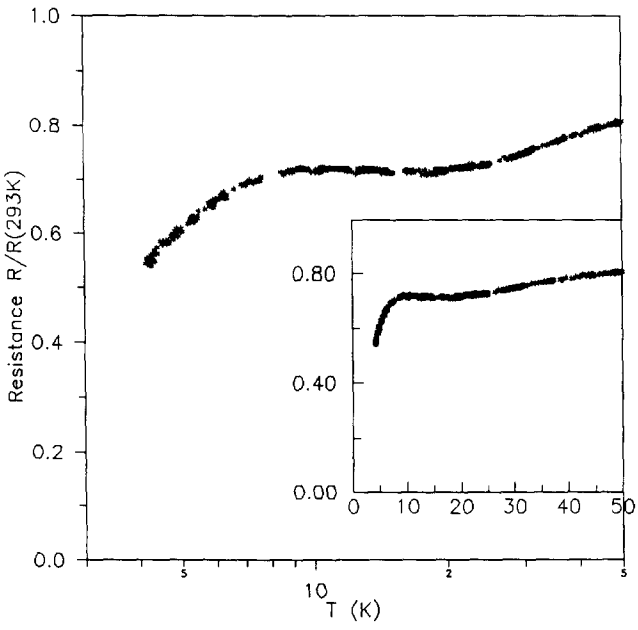

Fig. 3. Resistance ratio for Ce_2Ni_2Sn from 4.2 to 50 K.

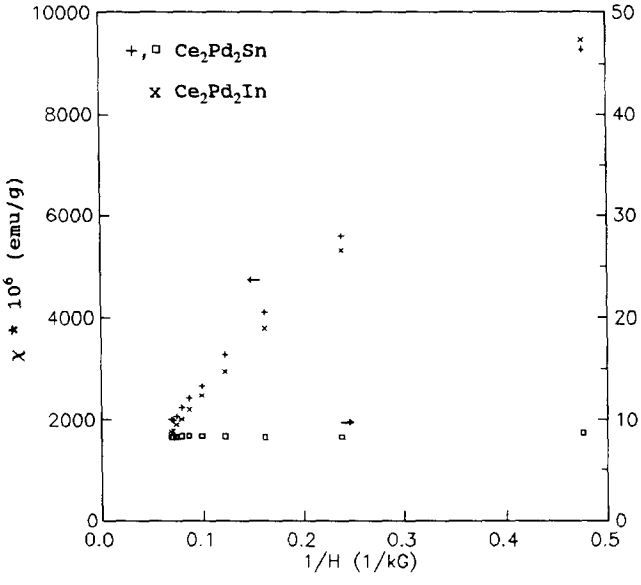

Fig. 4. Field dependence of the magnetic susceptibility for (×) Ce_2Pd_2In and (+) Ce_2Pd_2Sn at 4.2 K. For comparison, the field dependence of χ for (□) Ce_2Pd_2Sn at 308 K is also given.

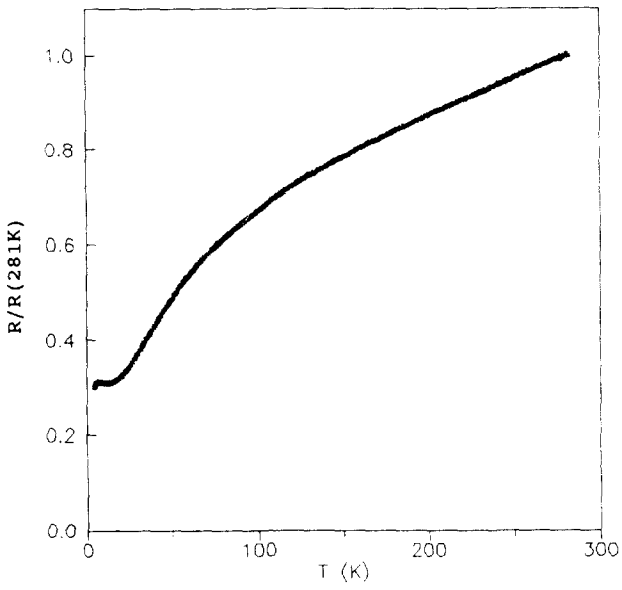

Fig. 5. Resistance ratio for Ce_2Pd_2Pb from 4.2 to 281 K. No obvious anomaly is observed near 120 K.

3.4. Ce_2Pd_2Sn

From the data shown in Fig. 2(f) and 2(g), a moment of 2.62 μ_B and ferromagnetic exchange ($\theta = 18$ K) can be determined, indicating that this material resembles ferromagnetic CePd more than the heavy fermion antiferromagnet, CePdSn. As for Ce_2Pd_2In, the field dependence of χ measured at 4.2 K (Fig. 4) for Ce_2Pd_2Sn exhibits a linear dependence on inverse magnetic field for high fields. Again, the ordering temperature can only be estimated as $T_c \approx 4.2$ K.

3.5. Ce_2Pd_2Pb

Above 120 K, Ce_2Pd_2Pb behaves in Curie–Weiss fashion (Fig. 2(h)) with a moment of 2.70 μ_B and antiferromagnetic exchange ($\theta = -30$ K). Below 120 K, the behaviour is, again, Curie–Weiss, but with reduced moment, 2.36 μ_B, and, apparently, with negligible exchange ($\theta \approx -1$ K). At lower temperature (<20 K), this compound undergoes anti-ferromagnetic ordering with a Néel temperature of 6.2 K.

By examining the inverse susceptibility (Fig. 2(i)) as a function of temperature, the nature of the transition at 120 K appears to be second order, based on the discontinuous change in slope. Resistance data (Fig. 5) obtained from a roughly 1 mm×2 mm×6 mm polycrystalline bar exhibit an anomaly at 6 K and a slow change in curvature above 20 K. Qualitatively, this behaviour resembles that for the anti-ferromagnet CePdSn [22]. The behaviour above 20 K can be understood in terms of some weak crystal field interactions. The anomaly near 6 K can be attributed to the antiferromagnetic ordering. No feature near 120 K was observed. The effect in susceptibility was reproduced in a second sample taken from the same arc-cast ingot as the bar used for resistance measurements. At this point, we do not understand the nature of this "transition".

4. Conclusions

We have prepared four new ternaries, Ce_2Ni_2Sn and Ce_2Pd_2M with M = In, Sn, Pb and we have studied the magnetic properties of these materials and the known ternary Ce_2Ni_2In. Cerium appears tetravalent in Ce_2Ni_2In, although the Pauli susceptibility is large and does exhibit some weak temperature dependence. An unusual peak in the susceptibility and Kondo-like behaviour in the resistance of Ce_2Ni_2Sn suggest Ce_2Ni_2Sn is a dense Kondo system. The three Pd phases possess trivalent cerium at room temperature. The Pd–In and Pd–Sn compounds exhibit ferromagnetic behaviour with T_c near 4.2 K, whereas the Pd–Pb phase shows antiferromagnetic ordering at 6.2 K and a transition at 120 K whose nature is at present unclear. Further attempts at electronic characterization are under way.

Acknowledgements

We acknowledge the support of the Office of Naval Research. We also thank M.E. Badding, M.D. Hornbostel and S.H. Elder for helpful advice during the early stages of this work.

References

[1] M. Kasaya, T. Tani, F. Iga and T. Kasuya, *J. Magn. Magn. Mater., 76/77* (1988) 278–280.
[2] T. Takabatake, F. Teshima, H. Fujii, S. Nishigori, T. Suzuki, R. Fujita, Y. Yamaguchi, J. Sakurai and D. Jaccard, *Phys. Rev. B, 41* (1990) 9607–9610.
[3] H. Fujii, T. Inoue, Y. Andoh, T. Takabatake, K. Satch, Y. Maeno, T. Fujita, J. Sakurai and Y. Yamaguchi, *Phys. Rev. B, 39* (1989) 6840–6843.
[4] R.V. Skolozdra and L.P. Komarovskaya, *Izv. Akad. Nauk SSSR Metally, 2* (1988) 214–218.
[5] E. Brück, M. van Sprang, J.C.P. Klaasse and F.R. de Boer, *J. Appl. Phys., 63* (1988) 3417–3419.
[6] To be published.
[7] G.L. Nieva, J.G. Sereni, M. Afyouni, G. Schmerber and J.P. Kappler, *Z. Phys. B Condensed Matter, 70* (1988) 181–186.
[8] P.E. Werner, L. Eriksson and M. Westdahl, *J. Appl. Crystallogr., 18* (1985) 367.
[9] Ya.M. Kalychak, V.I. Zaremba, V.M. Baranyak, P.Yu. Zavalii, V.A. Bruskov, L.A. Sysa and O.V. Dmytrakh, *Izv. Akad. Nauk SSSR Neorg. Mater., 26* (1990) 94–96.
[10] F. Mirambet, P. Gravereau, B. Chevalier, L. Trut and J. Etourneau, *J. Alloys Comp., 191* (1993) L1–L3.
[11] K. Yvon, W. Jeitschko and E. Parthé, *J. Appl. Crystallogr., 10* (1977) 73.

[12] D.L. Bish and R.C. Reynolds Jr., in D.L. Bish and J.E. Post (eds.), Mineralogical Society of America, 1989, *Reviews in Mineralogy*, Vol. 20, Chapter 4.

[13] V.A. Romaka, Yu.N. Grin and Ya.P. Yarmolyuk, *Ukr. Fiz. Zh., 27* (1982) 400–404.

[14] P.R. Bevington, *Data Reduction and Error Analysis for the Physical Sciences*, McGraw-Hill, New York, 1969.

[15] V. Sechovský, L. Havela, H. Nakotte, F.R. de Boer and E. Brück, *J. Alloys Comp., 207/208* (1994) 221–228.

[16] V.K. Pecharsky, O.-B. Hyun and K.A. Gschneider, Jr., *Phys. Rev. B, 47* (1993) 11839–11847.

[17] A good treatment of magnetic behaviour, including crystal field effects can be found in A.K. Cheetham and P. Day (eds.), *Solid State Chemistry: Techniques*, Oxford University Press, London, 1987, Chapter 4.

[18] F. Mirambet, B. Chevalier, L. Fournès, P. Gravereau and J. Etourneau, *J. Alloys Comp., 203* (1994) 29–33.

[19] C. Kittel, *Introduction to Solid State Physics*, Wiley, New York, 6th edn., 1986, Chapter 14.

[20] J.M. Ziman, *Principles of the Theory of Solids*, Cambridge University Press, Cambridge, 2nd edn., 1972, Section 10.5.

[21] R.M. White and T.H. Geballe, *Long Range Order in Solids*, Academic Press, New York, 1979, pp. 146–155.

[22] S.K. Malik, D.T. Adroja, S.K. Dhar, R. Vijayarghavan and B.D. Padalia, *Phys. Rev. B, 40* (1989) 2414–2418.

Note added in proof

Two of the phases discussed here, Ce_2Pd_2In and Ce_2Ni_2Sn have appeared in the *Journal of Alloys and Compounds*, Hulliger et al., *215* (1994) 267 and Fourgeot et al., *218* (1995) 90 respectively, since our work was submitted. Our results are consistent with those reported for these two compounds.